Gas Damping Model for a RF MEM Switch and its Dynamic Characteristics

Timo Veijola[1], Taisto Tinttunen[1], Heikki Nieminen[2], Vladimir Ermolov[2], and Tapani Ryhänen[2]

[1]Department of Electrical and Communications Engineering, Helsinki University of Technology, P.O.Box 3000, FIN-02015 HUT, Finland, E-mail:timo@aplac.hut.fi,
[2]Nokia Research Center, P.O. Box 407, FIN-00045 NOKIA GROUP, Finland

Abstract — **A compact model for a capacitive RF MEM switch with damping is presented. The damping model is based on analytic expressions for flow resistances due to the rarefied air flow in the gap and in the perforation holes. The complete switch model is constructed of elements resulting from the discretization of the beam deflection equation and has been implemented as a nonlinear electrical equivalent circuit. The model reproduces the beam displacement accurately. Comparison with measured transient on/off capacitance characteristics shows very good agreement.**

I. Introduction

The switching characteristics of a capacitive RF MEM switch are an important issue in several applications. The prediction of the switching times requires an accurate analysis of the whole switch structure, the dynamics of the mechanical structure, and the air flow. For accurate results when the device is switched on, it is necessary to include a realistic deflection profile of the bridge in the model.

A simple model af a capacitive MEM switch has been presented in [1]. It roughly imitates the device dynamics, but its parameters cannot be directly derived from the device structure. In [2], a switch model is presented, but a constant deflection profile is assumed.

A model for the static behaviour of a RF MEM switch is presented in [3]. It is based on a nonlinear electrical equivalent circuit model approach. The model has been constructed of elementary component models for beam deflection, electrostatic actuation force, gap capacitance, and mechanical contact.

In this paper, a novel nonlinear damper element is introduced and the switch model of [3] is augmented with this model. This damping model includes the nonlinear damping and spring forces due to the gas flow in the air gap and through the perforation holes.

Since the gap is very small in the studied device, and becomes even smaller when an actuation voltage is applied, it is essential to have the gas rarefaction modelled correctly, although the switch operates at atmospheric pressure. At 1 atm, the Knudsen number is 0.14 for a gap of 0.5 μm, predicting a reduction in the damping force due to rarefaction by at least 1.9.

II. Structure and Operation of the Switch

Figure 1 shows the structure of the RF switch studied. The bridge has been perforated to reduce the damping due to the air flow. When an actuation voltage is applied across the bridge and the bottom plate, the bridge will bend down increasing the capacitance of the switch. When the voltage is removed, the spring forces will return the bridge back to its initial position.

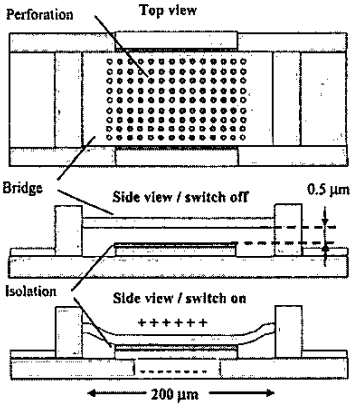

Fig. 1. Structure and the operation principle of the capacitive RF MEM switch. The switch is off when no DC voltage is applied (small capacitance). When a voltage larger than the pull-down voltage is applied, the brigde bends down and hits the dielectric layer (larger capacitance).

During the operation of the switch, the gas in the air gap will be squeezed into the perforation holes. This viscous flow is the cause of damping in the structure.

III. Switch Model

The differential equation modelling the motion of the bridge is

$$M\frac{\partial^2 z}{\partial t^2} + \gamma\frac{\partial z}{\partial t} + \tilde{E}I_y\frac{\partial^4 z}{\partial x^4} + h_b w_b S\frac{\partial^2 z}{\partial x^2} = q(x,z), \quad (1)$$

where z is the displacement, M is the mass of the beam, γ is the damping term due to the gas flow (not a constant term), $\tilde{E}$ is the effective Young's modulus, I_y is

0-7803-7239-5/02/$10.00 © 2002 IEEE

the moment of inertia, S is the stress in the beam, h_b and w_b are the height and width of the bridge, respectively, and $q(x,z)$ is the distributed load due to the electrostatic actuating force and the mechanical contact force.

A. Static Model

We have constructed a model for a RF MEM switch from elementary finite difference sections [3]. These sections consist of elements that model beam deflection, electrostatic actuation force, gap capacitance and mechanical contact force. The deflection model includes the contribution of both the static residual stress and the dynamic stress due to the elongation of the deflected beam.

Figure 2 shows how the switch model has been constructed. All but the two first and two last sections that implement the clamped-clamped beam boundary conditions are identical. The novel damper elements (PGD) are also shown in the figure. With this model, measured static capacitance-voltage-characteristics have been reproduced accurately [3].

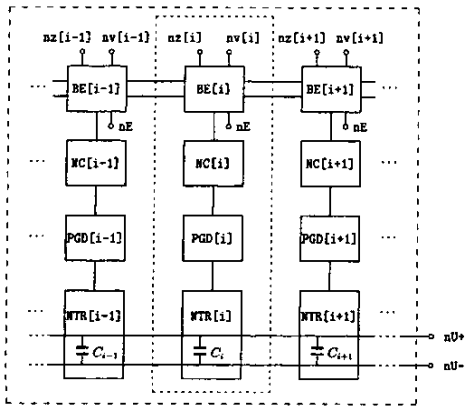

Fig. 2. Block diagram of the switch model. Each section contains a model for beam deflection (BE), mechanical contact (NC), gas damper (PGD), and electromechanical transducer (NTR) with electrostatic actuation force and cap capacitance. The capacitances of the sections are connected in parallel.

B. Model for Perforated Gas Damper

Mechanical losses in the bending bridge are low and the damping is dominated by the air flow. Here, it is assumed that the bridge has been perforated to reduce the damping due to air. In this case, we assume that the net horizontal flow under the bridge is zero: the gas flows entirely into the perforation holes from between the plates and the damping problem then reduces to a local flow problem in the vicinity of a single hole. Small pressure differences at the channel ends and a laminar flow are assumed.

Here, the validity of the model is limited to the regime where the gas inertia can be ignored. The measure of the validity is that the modified Reynolds number $\mathrm{Re} = \rho h^2 \omega / \eta \ll 1$, where h is the gap displacement, η is the viscosity coefficient, and ρ is the density of the gas. In the structure of interest, $\mathrm{Re} < 1$ for switching frequencies below 5 MHz.

C. Flow In the Gap

Flow from the air gap into the holes has been modelled by Skvor [4]. He assumes that the flow to each of the holes (radius r) enters from a cylindrical volume with radius r_x and height h, see Fig. 3. Parameter r_x has been determined according to [4], leading to a value of $2r_x = 1.13b$ where b is the distance between the centers of the holes. According to this model, the

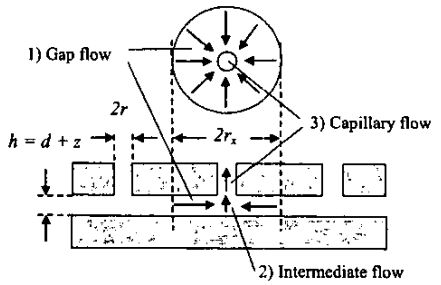

Fig. 3. The flow regimes around one perforation hole. It is assumed that the gas flows into each perforation hole from a cylindrical volume with a radius of r_x, and upwards through the perforation hole with a radius of r.

mechanical impedance R_s of a single hole is

$$R_s = \frac{2\pi D_{ch}\eta r_x^4}{Q_{p,ch}(D_{ch})h^3}\left(\frac{1}{2}\ln\frac{r_x}{r} - \frac{3}{8} + \frac{r^2}{2r_x^2} - \frac{r^4}{8r_x^4}\right), \quad (2)$$

where $h = d + z$ is the gap displacement, $Q_{p,ch}$ is the Poiseuille flow rate for the rectangular duct with a high aspect ratio. It is a function of the inverse Knudsen number $D_{ch} = \sqrt{\pi}/(2K_{n,ch}) = \sqrt{\pi}h/(2\lambda)$, where the Knudsen number is $K_{n,ch} = \lambda/h$ and λ is the mean free path of the gas, inversely proportional to pressure. In the continuum damping regime $Q_{p,ch}(D_{ch}) = D_{ch}/6$. An approximation for $Q_{p,ch}$ is [5]

$$Q_{p,ch}(D) = \frac{D}{6} + \frac{1.396}{D^{0.159}}. \quad (3)$$

The compressibility of the gas is modelled with a mechanical impedance

$$Z_s = \frac{1}{j\omega L_s} = \frac{(4r_x^2 - \pi r^2)P_A}{j\omega h} \quad (4)$$

where P_A is the pressure.

D. Flow Through the Perforation Holes

The vertical flow in the capillaries, formed by the perforation holes, is modelled with the flow resistance of a channel having a circular cross-section. The mechanical flow resistance for a long channel with circular cross-section (with radius r) is [5]

$$R_t = 2\pi l \frac{D_{tb}\eta}{Q_{p,tb}(D_{tb})} \tag{5}$$

where l is the channel length (thickness of the bridge), and $Q_{p,tb}$ is the Poiseuille flow rate, dependent on the inverse Knudsen number $D_{tb} = \sqrt{\pi}/(2K_{n,tb}) = \sqrt{\pi}r/(2\lambda)$, where the Knudsen number is $K_{n,tb} = \lambda/r$. In the continuum damping regime $Q_{p,tb}(D_{tb}) = D_{tb}/4$. An approximation for the flow rate $Q_{p,tb}$ is [5]

$$Q_{p,tb}(D) = \frac{D}{4} + 1.485\frac{1.78D + 1.}{2.625D + 1}, \tag{6}$$

E. Flow in the Intermediate Region

Analytic models for the flow between the surfaces and in the capillary exist, but the flow behaviour in the intermediate regime is too complicated to be analytically modelled. Here, this regime is approximated with elongations of the other flow channels.

Simple analytic expressions for effective elongation in rectangular and circular flow channels have been presented [5]. Here, the elongation of the channel flow under the bridge is modelled by increasing the radius r_x in Eq. (2) by

$$\Delta r_x = h\Delta L_{ch}(D_{ch}, (r_x - r)/h), \tag{7}$$

where the formula for the relative elongation is [5]

$$\Delta L_{ch}(D, L) = \frac{8}{3\pi}\frac{1 + 2.471D^{-0.659}}{1 + 0.5D^{-0.5}L^{-0.238}}. \tag{8}$$

The elongation of the capillary is modelled with a relative elongation ΔL_{tb} that depends on the inverse Knudsen number and the relative channel length l/r. The elongation is

$$\Delta l = r\Delta L_{tb}(D_{tb}, l/r), \tag{9}$$

where the formula for the relative elongation is [5]

$$\Delta L_{tb}(D, L) = \frac{3\pi}{8}\frac{1 + 1.7D^{-0.858}}{1 + 0.688D^{-0.858}L^{-0.125}}. \tag{10}$$

IV. Electrical Equivalent Circuit Implementation

The switch model has been constructed from elements that are built with electrical components, according to the inverse equivalencies [1], [6]. This approach uses node voltages to model velocities and displacements and controlled current sources to model actuation forces. Figure 2 shows the block diagram of the model, where nv[i] and nz[i] are the internal velocity and displacement nodes of elements i, and nU+ and nU- are the external capacitance nodes.

Figure 4 shows the equivalent circuit for a single damper element. Since inverse equivalencies are used, a gyrator is needed to transform the impedance circuit on the right-hand side of the figure into an admittance. The nonlinear resistance is $R_{ch} = R_s/(N_p N)$ where an effective radius $r_x + \Delta r_x$ is used instead of r_x, N_p is the number of perforation holes, and N is the number of elements. The compressibility effect in Eq. (4) is modelled with capacitor $C_{ch} = L_s/(N_p N)$.

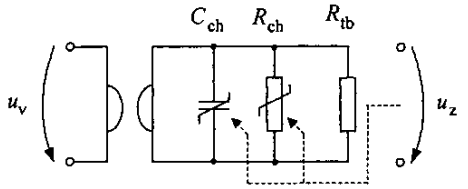

Fig. 4. Equivalent circuit element that models the mechanical admittance of the gas damper. The model contains the damping resistance due to the flow into the capillary R_{ch}, through the capillary R_{tb}, and the model for the gas compressibility C_{ch}. Nonlinear components R_{ch} and C_{ch} are controlled by the displacement u_z.

The flow resistance R_{ch} in the gap and the compressibility C_{ch} both depend on the displacement voltage u_z. In the gap flow model, also the elongation Δr_x and the inverse Knudsen numbers D_{ch} depend also on z.

The perforation hole resistance $R_{tb} = BR_t/(N_p N)$ is implemented as a constant resistance, since D_{tb} does not depend on the displacement z. In Eq. (5), the channel length $l + \Delta l$ is used instead of l. Coefficient B is utilized to scale the value of the capillary's resistance:

$$B = \frac{(r_x^2 - r^2)^2}{r^4} + 1. \tag{11}$$

The model has been implemented and simulated with the circuit simulation and design tool APLAC [7].

V. Experimental

Several capacitive MEM switches have been designed and fabricated. The structural material was gold; a silicon nitride dielectric layer isolates the suspended electrode from the bottom electrode. In addition, the process contains a third metal layer which is used as structural material in anchoring and to form coils. Dynamic on/off characteristics of a manufactured switch have been measured. The measurement setup is shown in Fig. 5. The capacitance as a function of time was measured using a self-made one-port vector network analyzer that operates at 836 MHz.

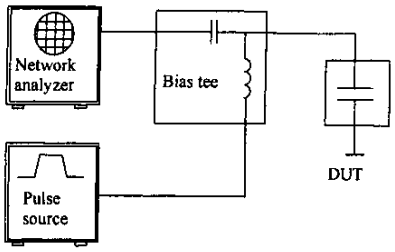

Fig. 5. Capacitance measurement setup for the MEM switch. A bias tee is used to separate the pulse voltage source from the network analyzer.

The static air gap height $d = 0.5\,\mu$m. The dimensions of the switch are the same as documented in [3]. The parameters in the dynamic model used here are exactly the same as in the CV characteristics simulations documented in [3]. Only the damper parameters have been added here, and no adjustments of the parameters have been made. The radius of the perforation holes is $2\,\mu$m and the ratio of the perforated area is 1/9. Air parameters at 1 atm have been used ($\lambda_{\text{air}} = 65$ nm, and $\eta_{\text{air}} = 18.5 \cdot 10^{-6}$ Nm/s^2). In the transient simulation, the beam was divided into $N = 100$ sections. Figure 6 shows the measured and simulated switch capacitance as a function of time when an actuation voltage pulse is applied to the switch.

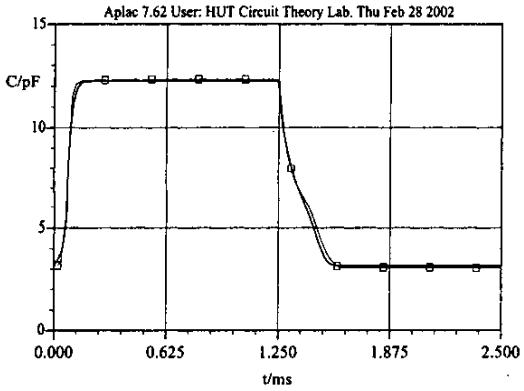

Fig. 6. Measured (—□—) and simulated (——) switch capacitance as a function of time when the DC voltage is switched on and off with an external actuation voltage of 3 V at a rate of 400 Hz.

VI. Conclusions

A circuit simulation model for a capacitive RF MEM switch was presented. A nonlinear damping model was derived for a perforated beam, and it was included in the static switch model. The damper model is based on analytic expressions for flow resistances due to the rarefied air flow into and through the perforation holes, and in the intermediate region [5]. Comparison with measured transient on/off capacitance characteristics shows very good agreement. The model presented is applicable also in simulating similarly constructed tunable capacitors.

Acknowledgement

The prototypes of the RF MEM capacitors were fabricated by Marjorie Trzmiel, Christian Pisella, and Stéphane Renard of Tronic's Microsystems, Grenoble, France.

References

[1] T. Veijola, "Nonlinear circuit simulation of MEMS components: Controlled current source approach," in *Proceedings of the 15th European Conference on Circuit Theory and Design*, (Espoo), pp. 377–380, Aug. 2001.

[2] J.-M. Huang, K. M. Liew, C. H. Wong, S. Rajendran, M. J. Tan, and A. Q. Liu, "Mechanical design and optimization of capacitive micromachined switch," *Sensors and Actuators A*, vol. 93, pp. 273–285, 2001.

[3] T. Tinttunen, T. Veijola, H. Nieminen, V. Ermolov, and T. Ryhänen, "Static equivalent circuit model for a capacitive MEMS RF switch," in *Proceedings of the 5th International Conference on Modeling and Simulation of Microsystems, Semiconductors, Sensors and Actuators*, (San Juan), Apr. 2002. Accepted for publication.

[4] Z. Skvor, "On the acoustic resistance due to viscous losses in air gap of electrostatic transducers," *Acoustica*, vol. 19, pp. 295–299, 1967.

[5] T. Veijola, "End effects of rare gas flow in short channels and in squeezed-film dampers," in *Proceedings of the 5th International Conference on Modeling and Simulation of Microsystems, Semiconductors, Sensors and Actuators*, (San Juan), Apr. 2002. Accepted for publication.

[6] T. Veijola and T. Mattila, "Modelling of nonlinear micromechanical resonators and their simulation with the harmonic balance method," *International Journal of RF and Microwave Computer-Aided Engineering*, vol. 11, pp. 310–321, 2001.

[7] M. Valtonen *et al.*, "APLAC - object-oriented circuit simulator and design tool," in *Low-Power HF Microelectronics - a Unified Approach* (G. Machado, ed.), ch. 9, IEE Circuits and Systems Series 8, IEE London, 1996.